

Phenomenological Characterization of the Electronically Enhanced Phase Noise in Transmission Experiments

Xiaoyan Ye, Amirhossein Ghazisaeidi, Sylvain Almonacil, Haik Mardoyan, Jérémie Renaudier

Nokia Bell Labs, Paris-Saclay, route de Villejust, Nozay, France, 91620 (xiaoyan.ye@nokia.com)

Abstract *We present a novel method based on parameter extraction to characterize the variance of the electronically enhanced phase noise in ultra-long haul WDM transmission experiments. Our method does not require an a priori knowledge of the laser phase noise characteristics.*

Introduction

Reduction of the cost-per-bit drives the coherent transponder industry to keep increasing the aggregate per-wavelength information rate of coherent detection transceivers. Recent single-carrier transceivers operate near 100 GBd, and the symbol-rate is expected to increase for the future generations. As the symbol-rate increases, the degrading impact of the electronically enhanced phase noise (EENP) on the overall system performance becomes more and more important, especially for ultra-long-haul terrestrial and submarine transmission [1]. The EENP originates from the filtering of the received signal after being beaten by the local oscillator (LO) field, which is contaminated by the phase noise [2-6]. The variance of the EENP linearly scales with the accumulated dispersion, (hence, with distance in dispersion unmanaged systems), baud-rate and laser phase noise. A theoretical analysis of the EENP variance, assuming the LO has Lorentzian shape, and that the EENP is additive, white and Gaussian is presented in [2], neglecting the impact of digital signal processing (DSP). However, it has been shown in [7] that the standard blind-phase search algorithm applied to estimate and track the optical phase in the coherent receiver, can partially mitigate the EENP, and its impact should not be ignored for accurate EENP characterization at high baud-rates [7,8]. More importantly, the Lorentzian hypothesis, which is equivalent to assuming that the power spectral density (PSD) of the frequency noise is flat over the observation window, does not hold for commercially available lasers. Given the growing importance of the EENP for modern coherent transponders, and the above-mentioned difficulties in providing closed-form accurate expressions for its variance, here we propose, for the first time to our knowledge, a new technique to phenomenologically characterize the EENP variance in transmission experiments, and to separate it from other main sources of noise, *i.e.*, the amplified spontaneous emission (ASE) noise, the Kerr nonlinear distortions, and the back-to-

back residual noise, without requiring to refer to the notion of Lorentzian linewidth, which is problematic to define and challenging to measure in practice

Theory of measurement

Our characterization technique is based on the following well-known expression [2] for the signal-to-noise ratio (SNR) of the signal at distance L , average power per channel P , and symbol-rate R :

$$SNR = \frac{P}{N_0LR + \eta(R)P + \sigma_{eepn}^2PLR + cP^3} \quad (1)$$

where, N_0 is the spectral level of the ASE, $\eta(R)P$ is the variance of the residual TRX noise in back-to-back, σ_{eepn}^2 is the EENP noise variance coefficient we aim to characterize in this work, and c is the Kerr nonlinear coefficient. To eliminate the dependence of the SNR to the variance of the residual TRX noise which does not depend on the transmission distance, we chose to derive the Eq (1) with respect to distance L . Let's define $s=1/SNR$, and consider

$$\frac{\partial s(P,L,R)}{\partial L} = \frac{N_0R}{P} + \sigma_{eepn}^2R + \frac{\partial c}{\partial L}P^2 \quad (2)$$

Which is called slope in the following. Starting from this equation to estimate the EENP noise variance, we propose to first measure the quantity s for various values of transmission distance L , and per-channel power P , and compute the approximate slope of s with respect to L based on the experimental data set. Finally, we propose to numerically fit the model of the slope vs. power as per Eq. (2) to the experimental slope vs. power curve and characterize the EENP noise variance σ_{eepn}^2 . Moreover, we repeat the same procedure for various values of R for the sake of checking the consistency of the measured results.

Experimental Results

The setup is shown in Fig. 1. The transmitted signal was synthesized using a WDM loading comb composed of 40 C-band DFB lasers

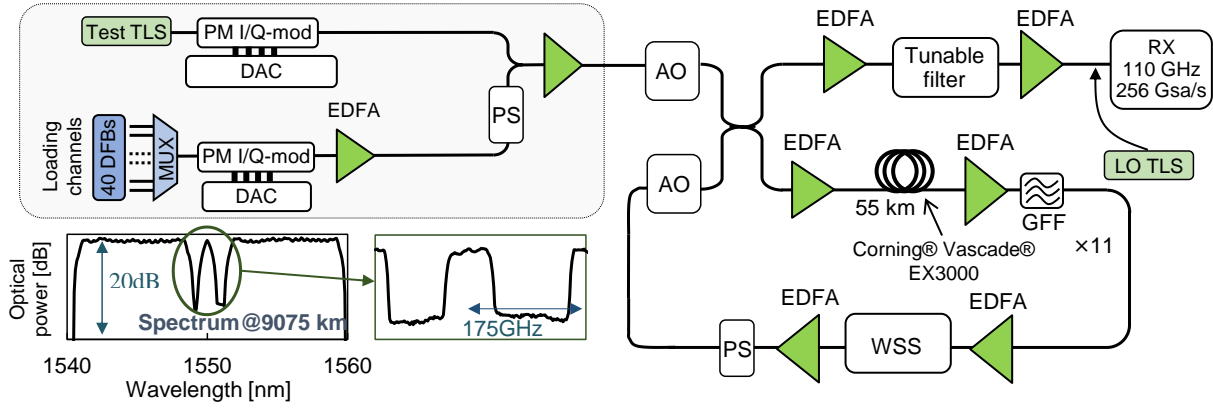


Fig. 1: Experimental setup. TLS: tuneable laser source; DFB: distributed feedback laser; DAC: digital-to-analog convertor; WSS: wavelength selective switch; PM I/Q-mod: polarization-multiplexed IQ modulator; A.O.: acousto-optic switch; PS: polarization scrambler; EDFA: erbium-doped fiber amplifier. Insets show the optical spectrum after 9075km.

spaced at 50 GHz, modulated with 49GBd PDM QPSK signals. The test channel is made of a tuneable laser source (TLS), separately modulated with PDM-QPSK signals at various symbol rates using a CMOS DAC operating at 120 GSamples/s. Digital pre-compensation is applied for the channel under test. The loading channels comb passed through a polarization scrambler (PS) before being multiplexed with the test channel. The test channel and the dummy WDM comb were multiplexed together and launched into the recirculation loop. This loop consisted of 11 spans of 55 km Corning EX3000 fibers, with 0.157 dB/km loss coefficient, $D = 20.5$ ps/nm/km dispersion coefficient at 1550 nm, and $150 \mu\text{m}^2$ effective area. The span loss was compensated at the end of each span by a C-band EDFA followed by a gain flattening filter (GFF). A 50 GHz-grid-resolution WSS was used after the last span of the loop to equalize WDM channels across the whole C-band. Each loop thus emulated transmission over 605 km. We then performed transmission experiments at different total launched powers ranging from 11 to 17 dBm which were repeated for three different symbol rates of 80 GBd, 85 GBd and 90 GBd. For each configuration of launch power and symbol rates, we measured the channel under test after 10 to 15 loops by steps of one loop, so as to

obtain distances ranging between 6050 and 9075 km by steps of 605km. The signal at the loop output was received by a standard coherent receiver front-end with another TLS used as LO in this work. The front-end signal is sampled at 256 GSamples/s using a 110 GHz real-time sampling scope, and the standard DSP is applied off-line to the recorded sampled waveforms^[10]. The standard DSP suite consisted of chromatic dispersion compensation, complex MIMO 2x2 constant modulus algorithm, frequency offset compensation, and blind phase search carrier phase recovery with 2% pilot overhead to remove cycle-slips, followed by a LMS equalizer to mitigate transmitter imperfections.

Next, the SNR of the received signals was calculated, the $s=1/SNR$ was obtained, and the approximate experimental slope vs. power was computed for each data set. We numerically extracted three parameters a , b , c to fit the model of Eq. (2). i.e., $\partial s/\partial L = a/P + b + cP^2$ to the measured slope vs. power curves.

Fig. 2 illustrates the PSD of the frequency noise of our LO TLS directly measured by a commercial optical phase noise test and measurement system. The PSD is clearly not flat over the observation window pertinent to the EEPN characterization, which is determined by the memory of the chromatic dispersion compensating filter. In time domain, and for $R = 90$ GBd (i.e., $\Delta\lambda = 0.72$ nm), at $L = 9075$ km the length of the impulse response of the CD filter is $DL\Delta\lambda \approx 133$ ns (~ 7.5 MHz⁻¹). This means that the PSD of the frequency noise should be integrated from 7.5 MHz onwards to obtain the variance of the phase noise of the LO under consideration here. This procedure allows us to estimate the actual frequency noise PSD by an equivalent constant level which results in the same area under the curve. The constant level is 14.7×10^3 Hz²/Hz for our TLS LO. Then, following [9], we multiply this value by 2π and find the equivalent

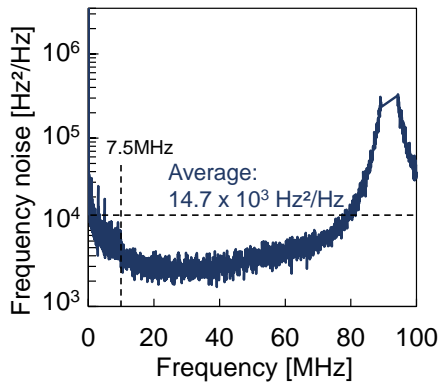


Fig. 2: The power spectral density (PSD) of the frequency noise of the TLS laser used as LO.

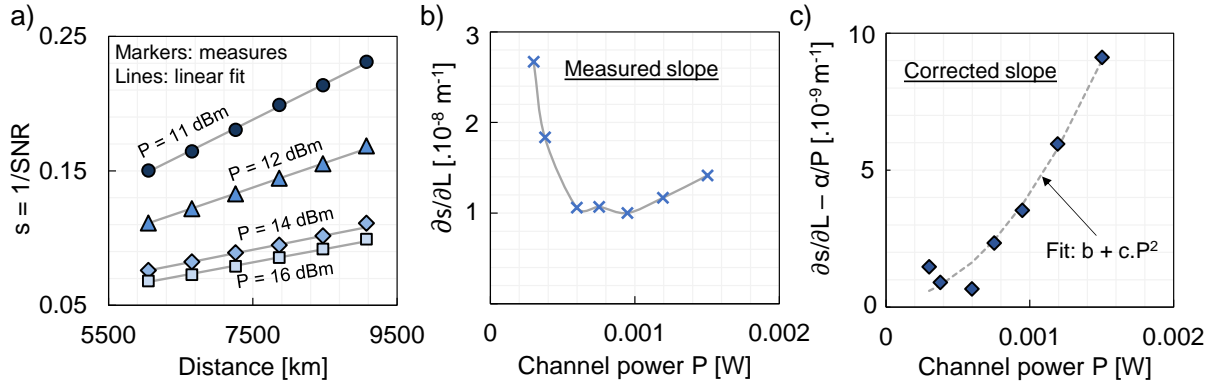


Fig. 3: a) s with respect to L , b) measured slope vs. channel power P , c) ASE-corrected slope with constant plus quadratic fit.

two-sided Lorentzian linewidth $\Delta\nu$ for our TLS LO. This can be used for comparison in the following well-known DSP-agnostic analytical expression for the variance of EEPN [2, 7]

$$\sigma_{eePN}^2 = \frac{\pi C D \Delta\nu}{2 f^2} \quad (3)$$

C is light speed, f is the optical carrier frequency.

Fig. 3a illustrates experimental s vs. distance curves for various powers, together with the linear fits in dashed lines using Huber cost function to suppress outliers' impact. The slope of these fitted lines is considered as the approximate experimental slope $\partial s / \partial L$.

Fig. 3b now illustrates the measured experimental slope vs channel power. We can see from this graph the evolution of the measured slope in the linear and slightly nonlinear regimes as a function of the channel power. To extract the EEPN noise variance as expected from Eq. (2), we proceeded in two steps. First, we exhaustively searched for a , such that the ASE-corrected slope: $\partial s / \partial L - a / P$ becomes as flat as possible for the powers corresponding to the linear regime below 14 dBm launch power (by minimizing the slope of the fitted line to the ASE-corrected slope). As for sanity check, we also measured the optical signal-to-noise ratio (OSNR) of the test channel using an OSA device for every single acquisition and checked that these OSNR were consistent with the ASE-corrected slopes, thus indicating that our model fitting approach is indeed accurate. For OSNR measurement, we removed two adjacent channels on each side of the signal spectrum, as in Fig. 1. Then we plotted in Fig. 3c the ASE-corrected slopes for the measured channel power at the baud rate of 85 GBd. As can be seen, the highest launched powers reveal the presence of nonlinearities as expected by the last term in Eq. (2). We finally interpolated the ASE-corrected slope according to a constant plus parabolic law in order to estimate the EEPN noise variance. Fig. 4 now shows the resulting EEPN noise variance estimated for our three measurements data sets at 80, 85 and 90 GBd. The EEPN noise variance obtained from the DSP-agnostic

analytical expression of Eq. (3) is also plotted for comparison. We can clearly see that the measured EEPN noise variances measured at the three symbol rates are consistent although well below the theoretical expectations taken from Eq. (3). This is consistent with our previous findings in [8]. Although there is a slight deviation among the estimated variances at different baud rates, we expect that the quality of estimation be

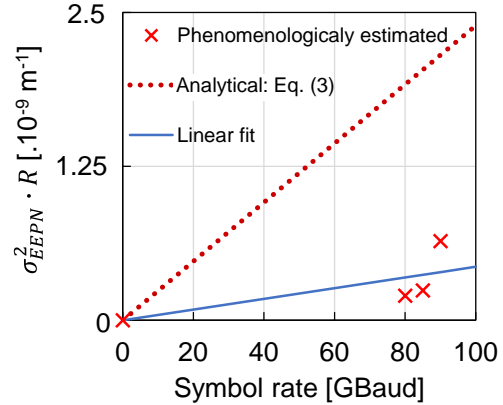


Fig. 4: Estimated EEPN noise vs. Baudrate

improved in future work when more data will be collected to enhance the accuracy.

Conclusions

We proposed a new method to characterize the value of the EEPN variance arising in WDM transmission experiments in linear and slightly nonlinear regime without a priori knowledge of the laser phase noise characteristics. Based on parameter extraction of a well-known analytical model for the evolution of the signal-to-noise ratio along the link, the technique is also independent from the transceiver imperfections. Experimental validation of the technique has been performed over a submarine testbed with transmission distances ranging from 6050 to 9075 km. With the growing importance of EEPN effect in modern coherent systems over ultra-long-haul distances, further improvement of the accuracy of the technique will be the subject of future works through the collection of more experimental data to enhance the accuracy of parameter extractions.

References

- [1] K. Benyahya, A. Ghazisaeidi, V. Aref, M. Chagnon, A. Arnould, S. Ranzini, H. Mardoyan, F. Buchali, J. Renaudier, "On the Comparison of Single-Carrier vs. Digital Multi-Carrier Signaling for Long-Haul Transmission of Probabilistically Shaped Constellation Formats," OFC 2021.
- [2] W. Shieh and K. Ho, "Equalization-enhanced phase noise for coherent detection systems using electronic digital signal processing," *Opt. Express*, vol. 16, no. 20, pp. 15718–15727, 2008.
- [3] C. Xie, "Local oscillator phase noise induced penalties in optical coherent detection systems using electronic chromatic dispersion compensation," presented at the Opt. Fiber Commun. Conf. Nat. Fiber Optic Engineers Conf., 2009, Paper OMT4.
- [4] I. Fatadin and S. J. Savory, "Impact of phase to amplitude noise conversion in coherent optical systems with digital dispersion compensation," *Opt. Express*, vol. 18, no. 15, pp. 16273–16278, 2010.
- [5] A. Kakkar et al., "Comprehensive study of equalization-enhanced phase noise in coherent optical systems," *J. Lightw. Technol.*, vol. 33, no. 23, pp. 4834–4841, Dec. 2015.
- [6] G. Colavolpe, T. Foggi, E. Forestieri, and M. Secondini, "Impact of phase noise and compensation techniques in coherent optical systems," *J. Lightw. Technol.*, vol. 29, no. 18, pp. 2790–2800, Sep. 2011.
- [7] A. Arnould and A. Ghazisaeidi, "Equalization Enhanced Phase Noise in Coherent Receivers: DSP-Aware Analysis and Shaped Constellations," *J. Lightw. Technol.*, vol. 37, no. 20, pp. 5282–5290, Oct. 2019.
- [8] A. Carbó Meseguer, A. Arnould, J.-C. Antona, A. Ghazisaeidi, P. Plantady, S. Dubost, A. Calsat, E. Awwad, J. Renaudier, V. Letellier, "Experimental characterization of equalization-enhanced phase noise in transoceanic transmission systems", ECOC 2019.
- [9] G. Di Domenico, S. Schilt, and P. Thomann, "Simple approach to the relation between laser frequency noise and laser line shape", *Applied Optics* 49, issue 25, 4801-4807, 2010.
- [10] A. Ghazisaeidi, A. Arnould, D. Le Gac, E. Awwad, P. Brindel, P. Pecci, O. Courtois, A. LeRoy, J. Renaudier, "Power efficient transmission of 320 Gb/s over 17545 km, and 560 Gb/s over 6050 km using 98 GBd QPSK and 64QAM and CMOS technology", ECOC 2019.